the, now, three independently re-refined structures, we must conclude that this feature is normal for this structure type and arises from the inability of the apparent valence method to handle atoms possessing lone pairs in highly anisotropic structural environments, such as Bi^{3+} in the Bi_2O_2 layer of Aurivillius phases.

In all of our previous calculations of AV's we have used the empirical parameters derived by Brown & Altermatt (1985). For the present calculations we retained their values of $r_0 = 2{\cdot}094$ Å for Bi^{3+}—O^{2-} but did not use their value of $r_0 = 1{\cdot}917$ Å for W^{6+}—O^{2-} for reasons discussed by Domenges, McGuire & O'Keeffe (1985). Instead we used $r_0 = 1{\cdot}900$ Å which we derived from simple perovskite-related W^{VI} containing oxides.

The authors wish to thank Dr A. C. Willis, Research School of Chemistry, ANU, for X-ray diffraction data collection, Dr L. R. Wallenberg, University of Lund, Sweden, for assistance with high-resolution electron microscopy and Mr R. Heady, ANU Electron Microscopy Centre, for assistance with scanning electron microscopy.

References

ALCOCK, N. W. (1970). *Acta Cryst.* A**26**, 437–439.
BRADLEY, C. J. & CRACKNELL, A. P. (1972). *The Mathematical Theory of Symmetry in Solids. Representation Theory for Point Groups and Space Groups.* Oxford: Clarendon Press.
BROWN, I. D. (1978). *Chem. Soc. Rev.* **7**, 359–376.
BROWN, I. D. (1981). *Structure and Bonding in Crystals*, Vol. II, edited by M. O'KEEFFE & A. NAVROTSKY, pp. 1–30. New York: Academic Press.
BROWN, I. D. & ALTERMATT, D. (1985). *Acta Cryst.* B**41**, 244–247.
COPPENS, P. & HAMILTON, W. C. (1970). *Acta Cryst.* A**26**, 71–83.
DOMENGES, B., MCGUIRE, N. K. & O'KEEFFE, M. (1985). *J. Solid State Chem.* **56**, 94–100.
DORRIAN, J. F., NEWNHAM, R. E., SMITH, T. K. & KAY, M. I. (1971). *Ferroelectrics*, **3**, 17–27.
MEULENAER, J. DE & TOMPA, H. (1965). *Acta Cryst.* **19**, 1014–1018.
NEWKIRK, H. W., QUADFLIEG, P., LIEBERTZ, J. & KOCKEL, A. (1972). *Ferroelectrics*, **4**, 51–55.
NEWNHAM, R. E., WOLFE, R. W., HORSEY, R. S., DIAZ-COLON, F. A. & KAY, M. I. (1973). *Mater. Res. Bull.* **8**, 1183–1195.
RAE, A. D. (1989). *RAELS89. A Comprehensivive Constrained Least-Squares Refinement Program.* Univ. of New South Wales, Australia.
RAE, A. D., THOMPSON, J. G. & WITHERS, R. L. (1990). *Acta Cryst.* A**46**(Suppl.), C-278–C-279.
RAE, A. D., THOMPSON, J. G., WITHERS, R. L. & WILLIS, A. C. (1990). *Acta Cryst.* B**46**, 474–487.
SHELDRICK, G. M. (1976). *SHELX*76. Program for crystal structure determination. Univ. of Cambridge, England.
THOMPSON, J. G., RAE, A. D., WITHERS, R. L. & CRAIG, D. C. (1991). *Acta Cryst.* B**47**, 174–180.
WATANABE, A. (1982). *J. Solid State Chem.* **41**, 160–165.
WITHERS, R. L., THOMPSON, J. G. & RAE, A. D. (1991). *J. Solid State Chem.* In the press.
WOLFE, R. W., NEWNHAM, R. E. & KAY, M. I. (1969). *Solid State Commun.* **7**, 1797–1801.
WOLFE, R. W., NEWNHAM, R. E., SMITH, T. K. & KAY, M. I. (1971). *Ferroelectrics*, **3**, 1–7.
YANOVSKII, V., VORONKOVA, V. & MILYUTIN, V. (1983). *Kristallografiya*, **28**, 316 319.

Acta Cryst. (1991). B**47**, 881–886

Neutron Powder Investigation of the Tetragonal to Monoclinic Phase Transformation in Undoped Zirconia

BY H. BOYSEN AND F. FREY

Institut für Kristallographie und Mineralogie, LMU München, Theresienstrasse 41, 8000 *München* 2, *Germany*

AND T. VOGT

Institut Laue–Langevin, BP 156, 38042 *Grenoble CEDEX, France*

(*Received* 25 *January* 1991; *accepted* 11 *July* 1991)

Abstract

The tetragonal (t) to monoclinic (m) transformation in pure ZrO_2 was investigated by neutron powder diffraction at temperatures between 1900 K and room temperature. The results of a Rietveld analysis are compared with a previous investigation of the $m \rightarrow t$ transformation. The $t \rightarrow m$ transformation takes place near 1200 K (implying a hysteresis of 300 K) and in a much smaller interval (about 150 K compared with about 600 K in the $m \rightarrow t$ case). There are no indications of a two-stage process as found for the $m \rightarrow t$ transformation. The structural parameters of the m phase depend only on temperature while those of the t phase differ at the same temperatures for the forward and reverse transformation. The temperature dependence of the lattice constants suggests an orientational relationship $\mathbf{a}_t \| \mathbf{a}_m^*$ and $\mathbf{c}_t \| \mathbf{b}_m$.

0108-7681/91/060881-06$03.00

There are no macrostrains whereas the overall microstrain behaviour is similar in both cases, *viz.* the large microstrains present in both phases are released within the transformation regime. An analysis of temperature factors and diffuse background suggest dynamical disorder in the *t* phase and static disorder in the *m* phase.

1. Introduction

Pure or doped (*e.g.* with Ca, Y, Mg, ...) zirconia ZrO_2 plays an outstanding role in modern science and technology, as illustrated by the enormous literature published over the last few years, and this is due to its exceptional properties. Some basic properties are intimately related to the phase transformations occurring in undoped ZrO_2. Depending on temperature, ZrO_2 exists in three different phases, monoclinic ($P2_1/c$), tetragonal ($P4_2/nmc$) and cubic ($Fm\bar{3}m$) at ambient pressure, and orthorhombic phase(s) exist at higher pressures.

We have investigated the crystallographic aspects of the monoclinic (*m*) $\leftrightarrow$ tetragonal (*t*) phase transformation by neutron powder diffraction. The results of the $m \rightarrow t$ transformtion have been reported in a previous paper (Frey, Boysen & Vogt, 1990) called (I) in the following, and in which relevant references to the subject are given. Here we report the corresponding results for the reverse $t \rightarrow m$ transformation which differs in various aspects. Comparison of the two transformation directions allows some general conclusions to be drawn concerning the transformation mechanism, although it has to be kept in mind that the results may be partly sample dependent. A dependence on particle size, microstructures *etc.*, as well as different behaviour in single crystals is well known (Subbarao, Maiti & Srivastava 1974).

2. Experiments and data evaluation

Experimental details, *i.e.* neutron powder diffractometer D2B/ILL HFR Grenoble, $\lambda = 1{\cdot}594$ Å, 60 μm powder, mirror furnace heating, and the data evaluation procedure, *i.e.* Rietveld refinement, are as described in paper (I). A fresh sample of the same charge as used in (I) was heated to 1900 K and measurements were carried out down to 1100 K before a final run at room temperature. Unfortunately, due to malfunctioning of the temperature-control equipment the sample was heated to 1350 K for 10 min between the measurements at 1270 and 1220 K. This may have caused slight anomalies in this temperature region, and these are therefore not discussed further (they do not, however, affect the general results).

To account better for the considerable background modulation at high temperatures manual linear interpolation has been used instead of fitting a six-parameter polynomial as in (I). A few test refinements of the data of (I) using this method did not change those results. Anisotropic temperature factors could be refined in all cases. Restrictions had to be imposed for the minority *t* phase at 1190 K and below, and the minority *m* phase at 1270 K, where the asymmetry parameter *P*, the parameter η of the pseudo-Voigt function and the occupation n_{Zr} were constrained to the values of the other phase, respectively. Examples of observed and calculated patterns are shown in Fig. 1. The difference plot represents the real background to show the modulation, *i.e.* difference = observed (total) − calculated (Bragg reflections only).

3. Results and discussion

The diagrams could only be fitted in space groups $P4_2/nmc$ and $P2_1/c$ for the *t* and *m* phases, respec-

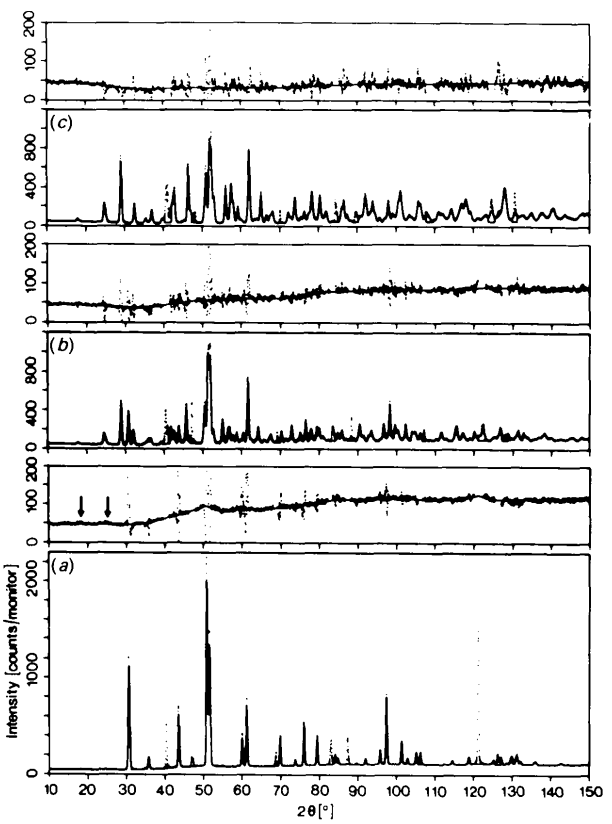

Fig. 1. Observed (dots) and calculated (solid line) powder patterns at (*a*) 1900 K, (*b*) 1270 K (*m* and *t* phase) and (*c*) 300 K (*m* only). Difference plots (dots) are shown separately and enlarged on top of each diagram together with the assumed background (solid line). Extra reflections are from the Pt sample container and were excluded from refinement.

tively, *i.e.* there are no other phases. At the highest temperature, 1900 K, only *t* reflections are observed although very faint and broad humps at the positions of the first strongest low-angle monoclinic reflections indicate the presence of some very small and disordered monoclinic embryos (*cf.* arrows in Fig. 1*a*). The deviations between observed and calculated intensities (Fig. 1) are mainly due to peak-shape problems caused by a non-Gaussian monchromator mosaic spread, which were not as severe in (I). This leads to rather poor profile *R* factors R_{wp}: around 10% when the *t* phase dominates and around 7% when the *m* phase dominates. Nevertheless there is confidence in the refined parameters, since positive and negative deviations partly cancel for each reflection. This is reflected in satisfactory Bragg *R* factors which are around 4% in both phases. The results are illustrated in Figs. 2–8.* The occupation factor of O has been refined leading to a constant value of 1·06 (1), *i.e.* independent of the phase or the temperature. The same value has been found in (I). Possible explanations have been discussed in paper (I). Also η and *P* were almost the same in all refinements.

Fig. 2 shows the variation of the scale factors of both phases. Short test runs, not suitable for a refinement, have been performed to detect the onset of the $t \rightarrow m$ transformation. At 1290 K such a measurement did not give any indication of monoclinic reflections. Therefore there is a rather sharp occurrence of the *m* phase. This contrasts with the findings for the $m \rightarrow t$ transformation where small amounts of the *t* phase are formed during an interval of about 300 K before the main transformation sets in. The main transformation itself takes place within about 150 K, compared with 300 K for $m \rightarrow t$. The overall hysteresis is about 300 K. Unfortunately, the limited beam time did not allow confirmation of a post-transformational region, which seems to be indicated by the slower decrease in the amount of *t* phase at 1100 K. The sum of both scale factors, *i.e.* the total amount of long-range ordered crystalline phases, slightly increases within the transformation region. This is counterbalanced by a decrease in the diffuse background, *i.e.* a small amount of somehow disordered material becomes well ordered in the course of the transformation.

Fig. 3 shows the variation of the lattice constants. We have again used a *C*-centred tetragonal cell for better comparison. Whereas the monoclinic lattice constants are nearly the same as found for the $m \rightarrow t$ transformation at the same temperatures, there are considerable deviations for the *t* phase. Down to 1200 K there is a 'normal' linear decrease below which both a_t and c_t decrease more rapidly. This contrasts with the behaviour in the $m \rightarrow t$ direction

* Lists of positional parameters, anisotropic thermal parameters, lattice constants, and scale and instrumental parameters have been deposited with the British Library Document Supply Centre as Supplementary Publication No. SUP 54414 (7 pp.). Copies may be obtained through The Technical Editor, International Union of Crystallography, 5 Abbey Square, Chester CH1 2HU, England.

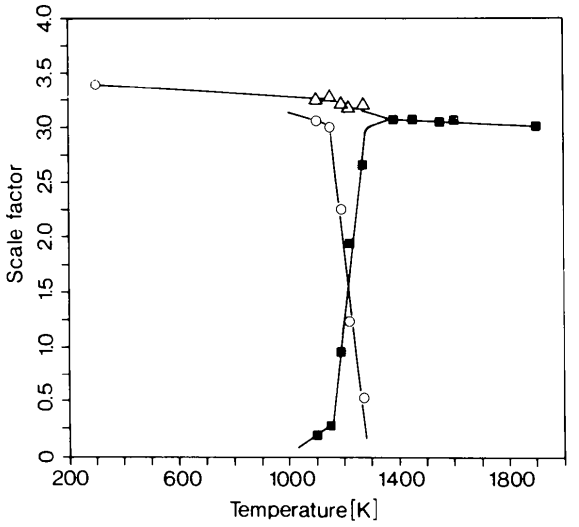

Fig. 2. Adjusted scale factors representing fractions of monoclinic (○) and tetragonal (■) phases during the transformation (total: △).

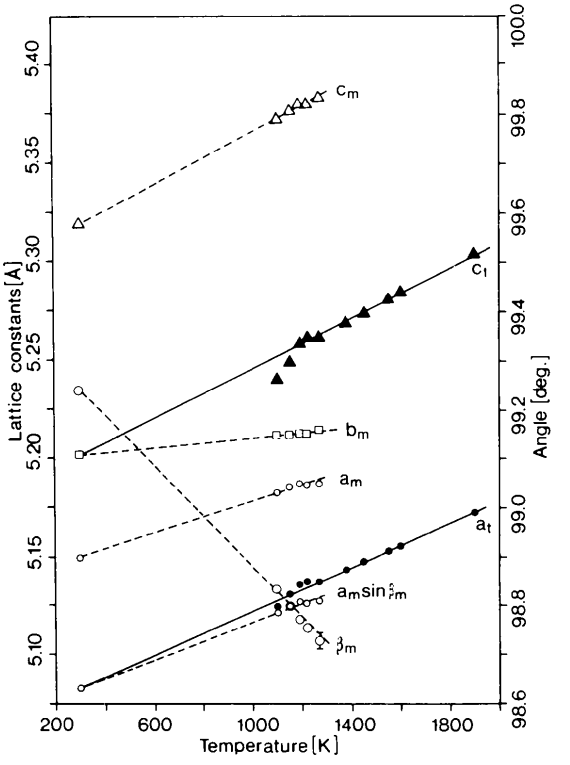

Fig. 3. Temperature dependence of the lattice constants. Note that a_t corresponds to a *C*-centred setting.

where the initially larger c_t and smaller a_t were assigned to a pre-transformational region, and only a small increase of both takes place during the main transformation. Extrapolation of the linear part of c_t and a_t to room temperature (see solid line in Fig. 3) clearly indicates a correspondence of c_t to b_m and a_t to $a_m \sin\beta_m$. The corresponding volume changes are shown in Fig. 4 together with the V_m:V_t ratio. Again V_m shows nearly the same temperature behaviour as in the $m \rightarrow t$ transformation. Slightly smaller absolute values might be attributed to a slight uncertainty in the calibration of the wavelength. The lack of the kind of saturation found for the $m \rightarrow t$ transformation suggests that there are no macrostrains during the main part of the $t \rightarrow m$ transformation. This also explains the slightly larger volume changes: $\geq 3{\cdot}5\%$ for $t \rightarrow m$ compared with $3{\cdot}2\%$ for $m \rightarrow t$ [compare Fig. 4 with Fig. 8 of paper (I)].

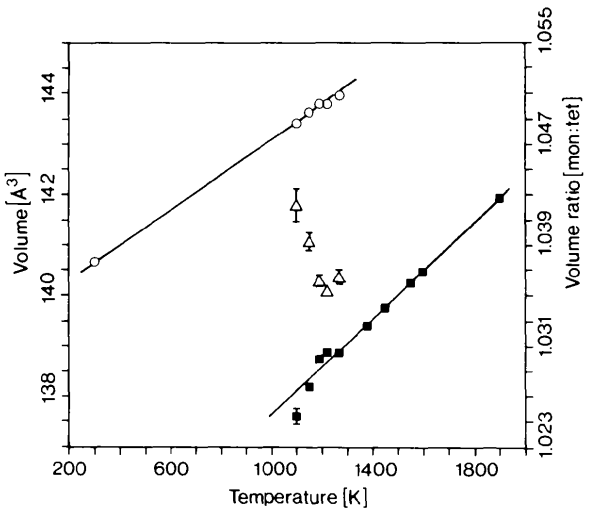

Fig. 4. Cell volumes (monoclinic: ○, tetragonal: ■) and volume ratio V_m:V_t (△) as functions of temperature.

Fig. 5 shows the variation of the positional parameters. In the monoclinic phase these have been plotted as the differences from their values in the tetragonal phase. These values agree with those of paper (I) within two standard deviations (e.s.d.'s), with the exception of x(O1) between 1100 and 1200 K (up to six e.s.d.'s). Hence, neglecting this deviation, the positional parameters of the m phase depend only on temperature, not on the direction of the transformation. This contrasts with the behaviour of the only free parameter in the t phase, z(O), which does not show the dramatic decrease with decreasing temperature as found in (I), but even shows a very slight increase (just over one e.s.d.). Together with the variation of the lattice constants this means that the two Zr—O bond lengths approach each other as the temperature is decreased,

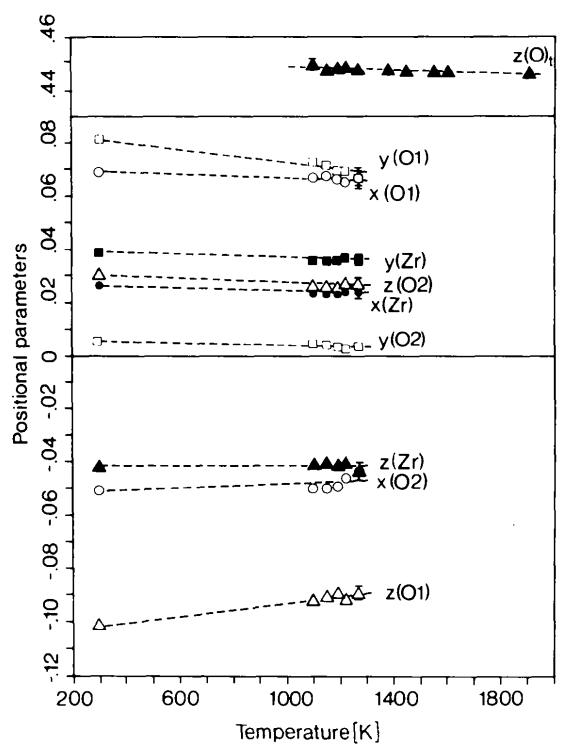

Fig. 5. Positional parameters of m and t phases. Fractional coordinates of the m phase are given as differences from their values in the tetragonal phase.

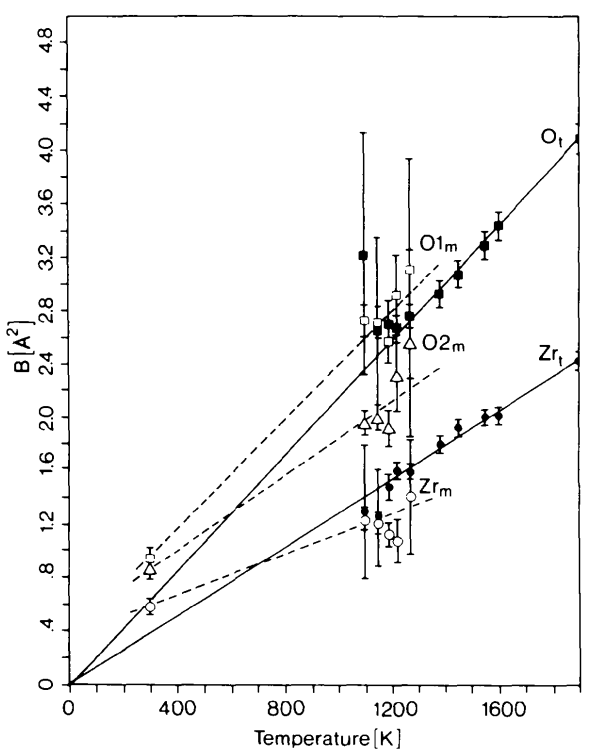

Fig. 6. Temperature dependence of the isotropic temperature factors (open symbols: monoclinic, closed symbols: tetragonal).

whereas the tetragonal distortion of the ZrO_8 polyhedra was much larger in the initial stages of the $m \rightarrow t$ transformation.

Fig. 6 shows the temperature dependence of (equivalent) isotropic temperature factors. Apart from $B(Zr_m)$ all temperature factors are slightly larger than in the $m \rightarrow t$ transformation, although the differences are not larger than three e.s.d.'s. The results for the t phase for both O and Zr define a straight line which readily extrapolates to zero at 0 K. Similar lines through the values of the m phase give finite values at 0 K indicating some static disorder in the m phase. The anisotropy of the thermal ellipsoids is similar to that described in (I) for both phases. As known from the previous results, the ellipsoids are elongated along ⟨110⟩ (Fig. 7).

As in the $m \rightarrow t$ transformation there is considerable variation in line widths. This has been analysed in terms of particle sizes and (micro)strains in paper (I). Unfortunately, owing to some changes to the monochromator mosaic, no purely instrumental values of U, V, W were at hand in this case. We therefore took the values of the lowest width *versus* 2θ curve (t phase at 1270 K) as reference. We do not claim any significance in the quantitative values, but restrict ourselves to the striking qualitative behaviour. The starting t phase at 1900 K as well as the final m phase at room temperature shows considerable strain (Fig. 8). As in the $m \rightarrow t$ case these strains are released approaching the transformation region. Again there is no indication of any particle-size broadening with the exception of the t phase at 1150 and 1100 K, where particle sizes of roughly 300 Å were found.

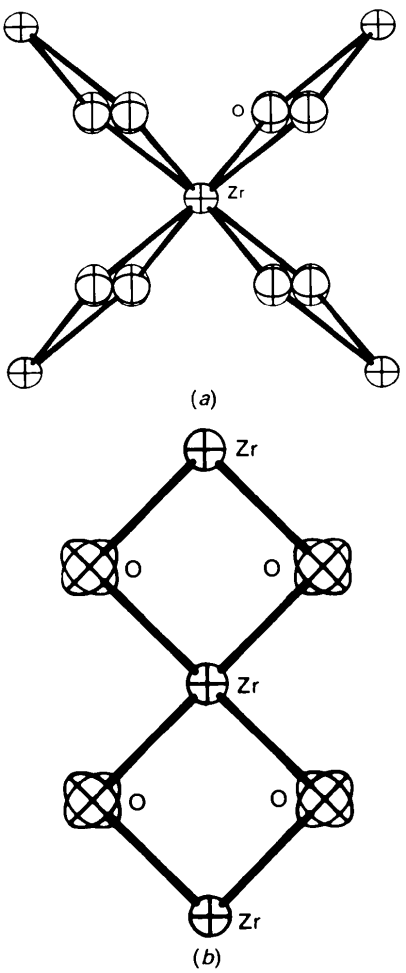

Fig. 7. Thermal ellipsoids at 1600 K in (*a*) (010), and (*b*) (001), projections.

4. Concluding remarks

Apart from the large hysteresis of about 300 K and the narrower transformation interval of the $t \rightarrow m$ transformation, there is a clear difference in the transformation process itself. Firstly, there is no precursor stage with a slow increase of m phase as found for the t phase in the $m \rightarrow t$ transformation. There is some indication of a post-transformational stage of small remaining t particles suggested by the slower decrease in the amount of t phase below 1150 K (Fig. 2), the deviations from linear temperature dependence of the lattice constants (Figs. 3, 4), the very large strains (Fig. 8), and the small particle sizes. These deviations from linearity in the residual t phase are very much the opposite of what is found in the pre-transformational stage during the $m \rightarrow t$ transformation (although occurring at roughly the same temperatures). Whereas during the $t \rightarrow m$ transformation all structural parameters show a 'normal' linear temperature dependence, strong non-linearity was found in the $m \rightarrow t$ direction. This shows that the

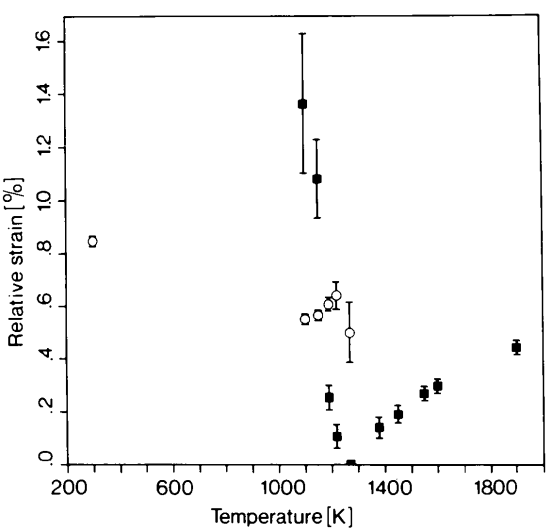

Fig. 8. Temperature dependence of microstrains.

parameters of the tetragonal structure are not a unique function of temperature, *i.e.* they depend on the direction of transformation. On the other hand, all parameters of the *m* phase having a normal linear temperature dependence in its range of existence are practically identical to those that occur during the $m \rightarrow t$ transformation at the same temperatures.

From extrapolating the *B* factors down to 0 K we deduce some static disorder is present in the *m* phase. The same procedure for the *t* modification gives no indication of such behaviour. On the other hand, the presence of a modulated diffuse background (in the stability range of the *t* phase) means that there is some kind of disorder which might therefore be of dynamic origin. We have no direct evidence for this, however, and clearly more experiments, in particular inelastic neutron experiments, are needed in order to clarify this point. There is evidence, however, that the tetragonal modification is intrinsically less 'rigid' than the monoclinic one. This is consequently important for the properties of ZrO_2-based materials.

In the paper (I) an orientational relationship $\mathbf{b}_t \| \mathbf{b}_m$ and $\mathbf{c}_t \| \mathbf{c}_m$ was suggested only for the precursor stage. Here we derived a different relationship, $\mathbf{c}_t \| \mathbf{b}_m$ and $\mathbf{a}_t \| \mathbf{a}_m^*$, from extrapolation of the lattice constants for the $t \rightarrow m$ transformation. Hence, it is not implausible that this relationship might also hold for the main part (second stage) of the $m \rightarrow t$ transformation. In fact, this conclusion could have been derived already from the earlier results [paper (I)]. It was not so clear, however, since only two points at the highest temperatures defined the linear temperature dependence in that experiment. Definite conclusions about orientational relationships are only possible by single-crystal experiments *via* inspection of the reciprocal lattices of coexisting *m* and *t* phases. Such an experiment has been carried out, but the results have not yet been evaluated (Mursic, Vogt, Frey & Boysen, 1991).

The similar behaviour of the microstrains in both cases favours the explanation given in paper (I), that they originate only from the specific microstructure of our sample and thus this probably rules out the other possibilities discussed in (I).

This work was supported by funds from the BMFT under project No. 03-SC2LMU3.

References

FREY, F., BOYSEN, H. & VOGT, T. (1990). *Acta Cryst.* **B46**, 724–730.

MURSIC, Z., VOGT, T., FREY, F. & BOYSEN, H. (1991). In preparation.

SUBBARAO, E. C., MAITI, H. S. & SRIVASTAVA, H. S. (1984). *Phys. Status Solidi A*, **21**, 9–40.

Acta Cryst. (1991). B**47**, 886–891

A Master Diagram for the Quick Localization of Possible Homogeneity Ranges of Adamantane-Structure Compounds

BY E. PARTHÉ*

Laboratoire de Cristallographie aux Rayons X, Université de Genève, 24 quai Ernest-Ansermet, CH-1211 Geneva 4, Switzerland

AND P. PAUFLER

Institut für Kristallographie, Mineralogie und Materialwissenschaft, FB Chemie/Kristallographie, Universität Leipzig, Scharnhorststrasse 20, O-7030 Leipzig, Germany

(*Received* 22 *March* 1991; *accepted* 25 *July* 1991)

Abstract

The composition ranges of adamantane-structure compounds are controlled by two valence-electron equations. Based on these rules a master diagram can be constructed which allows the quick localization of possible homogeneity ranges of adamantane-structure compounds in any binary or ternary diagram. These theoretical predictions are compared with the reported experimental results on the homogeneity range of the adamantane structure in the system Cu–In–Se. The experimental data agree with the predictions; however, a deviation has been reported in one case. Possible explanations are given for this exception which needs to be verified in the future by a single-crystal structure study.

* Holder of the Wilhelm–Ostwald Chair at the University of Leipzig during June and July 1990.

0108-7681/91/060886-06$03.00